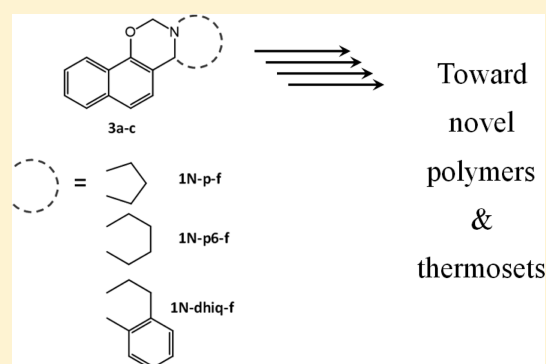


Design, Synthesis, Characterization, and Polymerization of Fused-Ring Naphthoxazine Resins

Carlos R. Arza,[†] Pablo Froimowicz,^{*,†,‡} Lu Han,[†] Robert Graf,[§] and Hatsuo Ishida^{*,†}[†]Department of Macromolecular Science and Engineering, Case Western Reserve University, Cleveland, Ohio 44106-7202, United States[‡]Design and Chemistry of Macromolecules Group, Institute of Technology in Polymers and Nanotechnology (ITPN), UBA-CONICET, School of Engineering, University of Buenos Aires, Av. Gral. Las Heras 2214 (PC C1127AAR), Buenos Aires, Argentina[§]Max Planck Institute for Polymer Research, Ackermannweg 10, D-55128 Mainz, Germany

ABSTRACT: Fused-ring naphthoxazine monomers are synthesized from 1-naphthols and cycloimines derived from piperidine and pyrrolidine. Their polymerization has been confirmed by differential scanning calorimetry (DSC), thermogravimetric analysis (TGA), and Fourier transform infrared spectroscopy (FT-IR) as well as by solution and solid-state ¹H and ¹³C nuclear magnetic resonance spectroscopy (NMR). A polymerization reaction similar to the traditional benzoxazine monomers is found with oxazine ring disappearing and hydroxyl group forming by the nonisothermal FT-IR experiment. Fused-ring monomers, studied in this work, polymerize at significantly lower temperatures compared to the ordinary benzoxazine resins.



INTRODUCTION

Polybenzoxazine is a new addition-type thermoset¹ that has aroused much scientific research interest² and has relatively recent been added to the list of commercially available thermoset materials³ because of their outstanding chemical, physical, and mechanical properties such as high thermal resistance⁴ including fully bio-based polybenzoxazines,⁵ resistance to flame,⁶ flexible molecular design,⁷ near-zero shrinkage,⁸ and very low surface free energy.⁹ The structural design flexibility of benzoxazine monomers is advantageous since the monomer synthesis utilizes widely commercially available phenols, primary amines, and formaldehyde.¹⁰ Less common methodologies have also been applied successfully for architectures where typical benzoxazine formation strategy, the Mannich condensation reaction, was incompatible. One of the most used pathways for the synthesis of these resins is the three-step strategy, which involves the formation of an open-Mannich base through the reaction of a primary amine and a 2-hydroxybenzaldehyde forming a Schiff's base as the first step. The second step involves the reduction of the Schiff's base usually with sodium borohydride and final closure of the ring with the use of formaldehyde (Scheme 1).¹¹ This strategy has been employed, i.e., for the formation of hydroxyl functionalized benzoxazine,¹² aminostyrene based benzoxazines,¹³ and cyanate ester containing benzoxazine.¹⁴

Polymers possessing naphthalene group are expected to exhibit excellent mechanical property and thermal stability, resulting from high backbone rigidity and aromatic content provided by the multiaromatic-ring structure. Previous works

have demonstrated the effectiveness of improving resin performance by incorporating naphthalene groups into backbone of various polymers, such as epoxy,¹⁵ PEEK,¹⁶ polyimide,¹⁷ poly(ϵ -caprolactone),¹⁸ and bismelamides.¹⁹ Compared to the wide range of studies in benzoxazine chemistry, naphthoxazines have received much less attention although some very interesting studies have been reported, including synthesis and mechanical study on aniline-based bifunctional naphthoxazines²⁰ and their degradation mechanism,²¹ thin film from telechelic naphthoxazine polymer,²² and thermal decomposition studies of aliphatic amine-based naphthoxazines and its polymer.²³ These limited activities are related in part to the easy evaporation of some naphthoxazine monomers during polymerization; however, chemical reactivity of naphthols is greater than that of phenols and thus could lead to advantageous synthesis conditions, such as monomer synthesis at room temperature.²⁴

Fused-ring naphthoxazines typically have a cycloaliphatic ring fused directly with oxazine ring, and they have been synthesized using 1-naphthol²⁵ or 2-naphthol^{26,27} as phenolic precursor with many alternative pathways for different organic chemistry studies. Despite the possibility of adding a great number of a new class of benzoxazines that can potentially lead to new polybenzoxazines, no study has yet been reported on the successful polymerization of fused-ring benzoxazines or

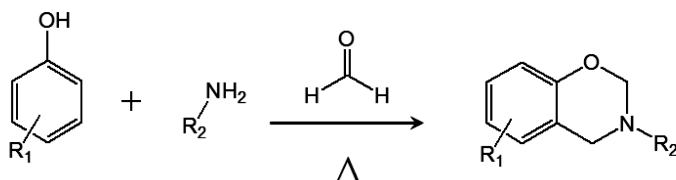
Received: May 5, 2017

Revised: November 7, 2017

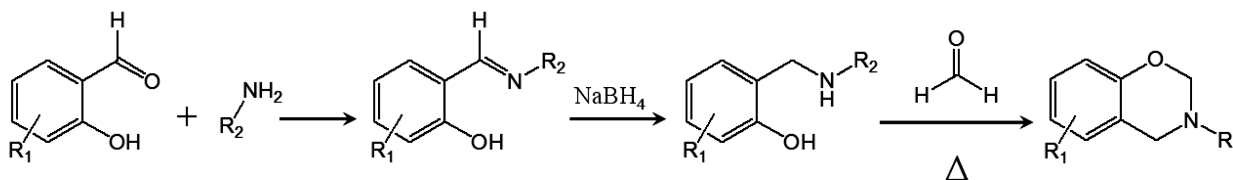
Published: November 20, 2017

Scheme 1. Synthesis of 1,3-Benzoxazines through (a) the One-Pot Modified Mannich Reaction of a Phenol, Primary Amine, and Formaldehyde and (b) the Three-Step Strategy

a) *one-pot modified Mannich reaction*



b) *three-step strategy*



naphthoxazines. Therefore, we developed an interest in studying if such compounds might be considered and even used as resins toward the generation of novel thermosets. Thus, as a starting point, we tackled in this work one of the many possible systems, specifically 1-naphthol-based fused-ring naphthoxazines. This initial selection of the herein studied resins was fundamentally based and supported by the reported superior performance of 1-polynaphthoxazines over 2-polynaphthoxazines.²⁰ To our knowledge, there are no previous reports on the polymerization of this class of fused-ring naphthoxazines, neither on the thermal stability of their resulting polymers. Thus, it is the purpose of this paper to study the feasibility of the polymerization of these fused-ring naphthoxazines rather than showing excellent properties of the resulting polymers. It is widely known that mono-oxazine benzoxazines and naphthoxazines do not lead to mechanically attractive properties due to the small oligomer formation. However, development of novel materials exhibiting better properties based on this new approach will be reported in time elsewhere.

EXPERIMENTAL SECTION

Materials. 1-Naphthol (for synthesis) was purchased from EMD Millipore. *N*-Chlorosuccinimide (98%), piperidine (99%), pyrrolidine (99%), sodium methoxide (25 wt % in methanol), sodium thiosulfate (99%), and 1,2,3,4-tetrahydroisoquinoline (95%) were used as received from Sigma-Aldrich. Acetonitrile, alumina, cyclohexane, dichloromethane (DCM), diethyl ether, formaldehyde solution (37% wt. in water), hexane, anhydrous magnesium sulfate (MgSO₄), sodium chloride (NaCl), sodium hydroxide (NaOH), and toluene were obtained from Fisher Scientific. Ordinary compounds used were of chemical reagent grades and utilized without further purification. Synthesis of imines **1a–c** were prepared following a reported method.²⁸

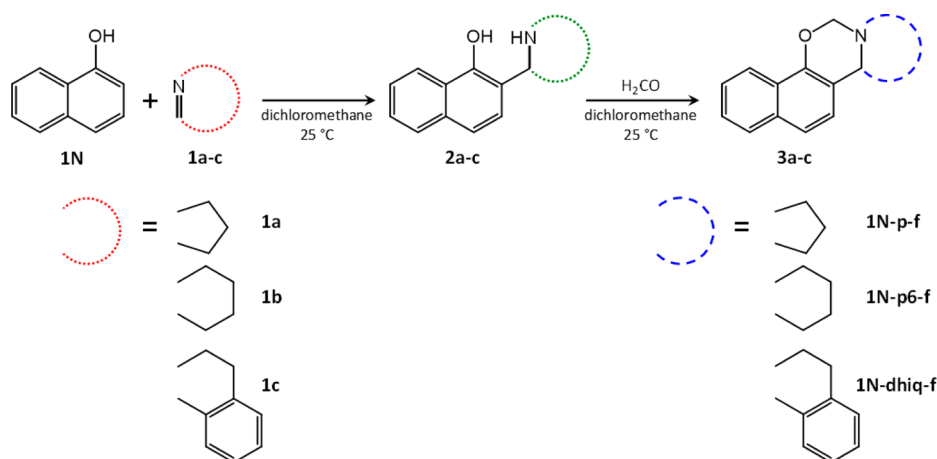
Synthesis of 8,9,10,10a-Tetrahydro-6*H*-naphtho[2,1-*e*]pyrrolo[1,2-*c*][1,3]oxazine (Abbreviated as 1*N*-p-f). Betti reaction for the formation of aminocycloalkylnaphthol was conducted by following the procedure as described.²⁹ A solution of **1a** (0.284 g, 4.11 mmol, 1.2 equiv) in DCM (3 mL) was added to a solution of 1-naphthol (0.494 g, 3.43 mmol) in DCM (3 mL). The reaction mixture was magnetically stirred in a sealed 15 mL vial at room temperature for

15 h. After evaporation of the solvent, diethyl ether (20 mL) was added; the organic phase was washed with a 0.5 N NaOH aqueous solution (3 × 5 mL) as well as brine (2 × 5 mL) and dried over MgSO₄. The solvent was removed, and the resulting product was dissolved in DCM (6 mL) and used without further purification, to which formalin (37 wt % aqueous solution, 0.83 mL, 10.3 mmol, 3 equiv) was added dropwise. The reaction mixture was stirred at room temperature overnight. After evaporation of the solvent, mixed hexane isomers (hexanes) (30 mL) were added, and the resulting suspension was filtered through a pad of alumina. Removal of the solvent afforded a transparent oil which crystallized on standing at low temperature (yield: 55%). ¹H NMR (600 MHz, CDCl₃, 20 °C) δ , ppm: 8.15 (d, 1H, Ar), 7.74 (s, 1H, Ar), 7.47 (m, 2H, Ar), 7.10 (d, 1H, Ar), 5.12 (d, 1H, O-CH₂-N), 5.07 (d, 1H, O-CH₂-N), 4.76 (bb, 1H, Ar-CH-(CH₂)-N), 3.23–1.78 (m, 6H, -N-CH₂-CH₂-CH₂-CH-(CH₂)-). FT-IR ν (cm⁻¹): 2968–2876 (C-H alkane str), 1325 (O-CH₂-N wagg), 1240 (C-O antisym str), 1198 (C-N antisym str), 1049 (C-O sym str), and 924 (oxazine-related band). HRMS (EI) m/z , [M]⁺ calculated for C₁₅H₁₅NO⁺: 225.11536; found: 225.11548.

Synthesis of 9,10,11,11a-Tetrahydro-6*H*,8*H*-naphtho[2,1-*e*]pyrido[1,2-*c*][1,3]oxazine (Abbreviated as 1*N*-p6-f). A mixture of 1-naphthol (0.99 g, 6.87 mmol) and **1b** (0.57 g, 6.87 mmol, 1 equiv) in DCM (14 mL) was stirred at room temperature for 24 h. The organic phase was washed with 0.5 N NaOH aqueous solution (3 × 15 mL) followed by water (2 × 15 mL). After removal of solvent, the resulting mixture was dissolved in 20 mL DCM, and formalin (37 wt % aqueous solution, 0.61 mL, 7.56 mmol, 1.1 equiv) was added. The reaction mixture was stirred at room temperature in a 50 mL round-bottom flask for 12 h. Then solvent was evaporated, and 50 mL of hexanes was added to the mixture. The resulting suspension was filtered through an alumina pad. The final product was obtained as a yellow solid (yield: 74.2%). ¹H NMR (600 MHz, CDCl₃, 20 °C) δ , ppm: 8.15 (dd, 1H, Ar) 7.75 (dd, 1H, Ar) 7.45 (m, 2H, Ar), 7.40 (d, 1H, Ar), 7.23 (d, 1H, Ar), 4.97 (d, 1H, O-CH₂-N), 4.86 (d, 1H, O-CH₂-N), 4.13 (bb, 1H, Ar-CH(CH₂)-N), 3.02–1.56 (m, 8H, -N-CH₂-CH₂-CH₂-CH₂-CH(CH₂)-). FT-IR ν (cm⁻¹): 2939–2748 (C-H alkane str), 1333 (O-CH₂-N wagg), 1242 (O-C antisym str), 1196 (C-N antisym str), 1055 (C-O sym str), and 916 (oxazine-related band). HRMS (EI) m/z , [M]⁺ calculated for C₁₆H₁₇NO⁺: 239.13101; found: 239.13130.

Synthesis of 9,13b-Dihydro-6*H*,8*H*-naphtho[2',1':5,6] [1,3]-oxazino[4,3-*a*]isoquinoline (Abbreviated as 1*N*-dhiq-f). A solution of **2c** (0.14 g, 1.07 mmol 1.2 equiv) in DCM (2 mL) was

Scheme 2. Synthesis of Fused-Ring Naphthoxazines



added to a solution of 1-naphthol (1.29 g, 0.89 mmol). The reaction mixture was stirred for 24 h at room temperature in a sealed 15 mL vial. After evaporation of the solvent, diethyl ether (10 mL) was added; the organic phase was washed with a 0.5 N NaOH aqueous solution (3 × 5 mL) as well as brine (2 × 5 mL) and dried over MgSO₄. Then, the solvent was removed, and the resulting product was dissolved in DCM and used without further purification. To the above mixture in a 15 mL vial, formalin (37 wt % aqueous solution, 0.26 mL, 3.21 mmol, 3 equiv) was added dropwise. Then the vial was sealed, and the reaction mixture was magnetically stirred at room temperature overnight. After removal of the solvent, the crude product was washed with ethanol and acetone. Recrystallization in acetone afforded light orange-white crystals (yield: 64%). ¹H NMR (600 MHz, CDCl₃, 20 °C) δ, ppm: 8.20 (dd, 1H, Ar), 7.71 (dd, 1H, Ar), 7.48–7.42 (m, 3H, Ar), 7.33 (t, 1H, Ar), 7.28 (dt, 1H, Ar), 7.26 (d, 1H, Ar), 7.21 (d, 1H, Ar), 7.20 (d, 1H, Ar), 5.60 (d, 1H, Ar–CH(Ar)–N), 5.50 (d, 1H, O–CH₂–N), 5.22 (d, 1H, O–CH₂–N), 3.34–2.76 (m, 4H, N–CH₂–CH₂–Ar). FT-IR ν (cm⁻¹): 2988–2833 (C–H alkane str), 1331 (O–CH₂–N wagg), 1246 (C–O antisym str), 1192 (C–N antisym str), 1065 (C–O sym str), and 920 (oxazine-related band).

Characterization. Proton nuclear magnetic resonance (¹H NMR) spectra were acquired on a Varian Oxford AS600 at a proton frequency of 600 MHz. The average number of transients for ¹H NMR measurement was 32. A relaxation time of 10 s was used for the integrated intensity determination of ¹H NMR spectra. Fourier transform infrared (FT-IR) spectra were recorded using a Bomem Michelson MB100 FT-IR spectrometer equipped with a deuterated triglycine sulfate (DTGS) detector and a dry air purge unit. Co-addition of 64 scans was recorded at a resolution of 4 cm⁻¹. A TA Instruments differential scanning calorimeter (DSC) Model 2920 was used with a heating rate of 10 °C/min and a nitrogen flow rate of 60 mL/min. All samples were sealed in hermetic aluminum pans. Thermal decomposition of the reacted materials was determined by thermogravimetric analysis (TGA) using a TA Instruments Model Q500 TGA. The TGA analysis was performed in a single heating run from room temperature to 900 °C at a heating rate of 10 °C/min, with a nitrogen flow rate of 60 mL/min. Size exclusion chromatography (SEC) was performed on a TOSOH GPC instrument equipped with Bryce-type double-path RI detector, UV-8320 detector, and miniDAWN TREOS three-angle light scattering detector. The stationary phase was TSKgel SuperMultiporeHZ-M HPLC column maintained at 35 °C. The SEC mobile phase was HPLC grade THF at a flow rate of 0.35 mL/min. The column set was calibrated against polystyrene (TOSOH, Japan). High-resolution mass spectrometry (HRMS) analyses were conducted on a KRATOS ms25 mass spectrometer, using electron impact (EI) as ionization source at 140 °C, electron energy of 28 eV, and in positive mode. Solid State NMR measurements have been performed at ambient conditions with a Bruker Avance III console operating at the proton Larmor frequency of 700.25 MHz using a commercial 2.5 mm double resonance magic

angle spinning (MAS) NMR probe. The experiments were conducted at ambient conditions and the MAS frequencies up to 35 kHz. ¹H MAS NMR spectra have been acquired with 16 transients at the 30 kHz MAS spinning frequency and 100 kHz radio frequency nutation for direct excitation. ¹³C cross polarization (CP) experiments have been performed at the MAS frequency of 25 kHz with a CP contact time of 1 ms, 20000 transients, and swept frequency two-pulse phase modulation (TPPM) high power ¹H decoupling during acquisition.

RESULTS AND DISCUSSION

In this study, in addition to the aforementioned modified Mannich reaction and three-step reactions in the Introduction section, another stepwise reaction is employed which gives rise to a novel type of benzoxazine-like resin namely fused-ring naphthoxazines. This approach involves the formation of first aminocycloalkylphenols by the Betti reaction of cyclic imines and activated phenols, followed by closure of the ring with formaldehyde.²⁹

The fused-ring naphthoxazines synthesized in this study are prepared by using 1-naphthol as activated phenols and compounds **1a–c** as the cyclic imines (Scheme 2). The formation of aminocycloalkylphenols is carried out under mild conditions and affords the desired product with good yields. Closure of the ring is a straightforward reaction that is easily accomplished with formaldehyde at room temperature. All chemical structures were confirmed by ¹H NMR. Figure 1 shows the ¹H NMR spectrum and numbering of the positions that are mentioned throughout this study using **1N-p-f** as an example. The numbering of the positions on the oxazine ring are given by pure numbers respecting the benzoxazine nomenclature, on the naphthalene portion of the molecule following the naphthalene nomenclature using a number accompanied by the character “n” for naphthalene, and finally the fused ring using alphabetic letters (a, b, and c in the example shown).

Unlike typical 1,3-oxazine protons in the oxazine ring which usually appear as singlets, the proton signals of the oxazine moiety in the fused-ring naphthoxazine ring at the 2-position emerged as two different signals. This is caused by the more rigid twisted-semichair conformation of the fused-ring naphthoxazine compared to ordinary benzoxazines and is attributable to the two simultaneous rings attached to each side of the oxazine ring, leading to an inhomogeneity of the magnetic environment for each proton of the oxazine CH₂ group.

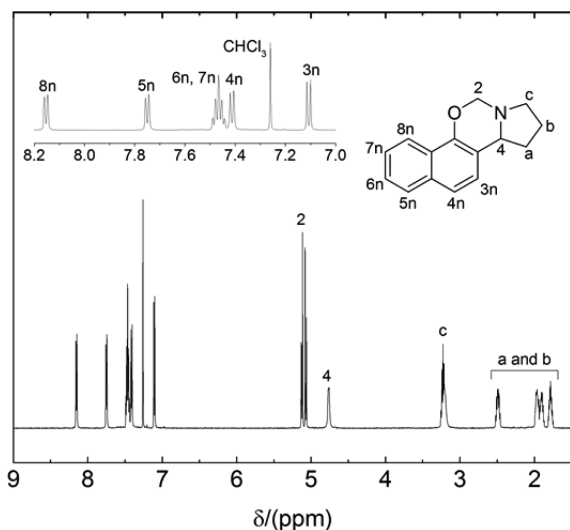


Figure 1. ^1H NMR spectrum and molecular structure of **1N-p-f** and the numbering of its positions using pure numbers for the oxazine positions (2 and 4), number accompanied by the character “n” for naphthalene on the naphthalene moiety, and finally alphabetic letters for the ring fused to the oxazine ring. The spectrum shown as an inset is an expanded view of the aromatic proton region.

The structures of the synthesized fused-ring naphthoxazines were also confirmed by FT-IR analysis. **Figure 2** shows the FT-

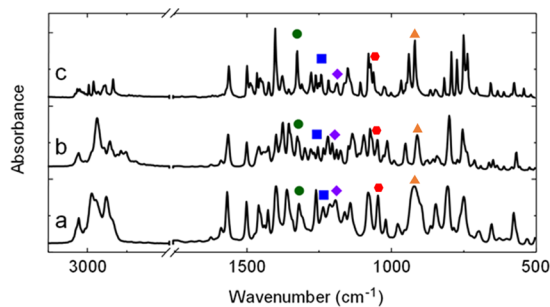


Figure 2. FT-IR spectra of (a) **1N-p-f**, (b) **1N-p6-f**, and (c) **1N-dihq-f**. Colored asterisks indicate characteristic modes for oxazine ring: $-\text{CH}_2$ wagging (●), C–O antisymmetric str (■), C–N antisymmetric str (◆), C–O symmetric str (●), and oxazine ring mode (▲).

IR spectra of **1N-p-f**, **1N-p6-f**, and **1N-dihq-f** with characteristic bands of the oxazine ring modes highlighted. **Table 1** summarizes the characteristic values for CH_2 wagging, Ar–O–C symmetric and antisymmetric stretching, C–N antisymmetric, and the oxazine ring mode.

In addition, **Figure 3** shows the FT-IR spectra of fused-ring naphthoxazines in the $1000\text{--}500\text{ cm}^{-1}$ region. The bands in the region of $900\text{--}650\text{ cm}^{-1}$ are associated with out-of-plane C–H

Table 1. Characteristic Vibration Frequencies for Oxazine Ring of Fused-Ring Naphthoxazines

| compound | vibration frequency (cm^{-1}) | | | | |
|------------------|--|-------------|-------------|---------|----------------------|
| | CH_2 wagg | C–O antisym | C–N antisym | C–O sym | oxazine-related band |
| 1N-p-f | 1325 | 1240 | 1198 | 1049 | 924 |
| 1N-p6-f | 1333 | 1242 | 1196 | 1055 | 916 |
| 1N-dihq-f | 1331 | 1246 | 1192 | 1065 | 920 |

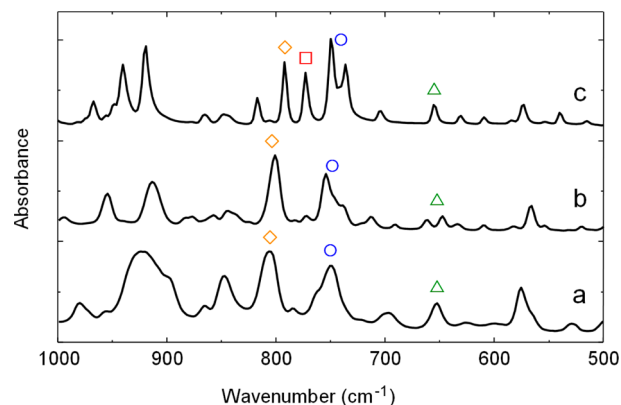


Figure 3. FT-IR spectra of (a) **1N-p-f**, (b) **1N-p6-f**, and (c) **1N-dihq-f**. Colored asterisks indicate characteristic C–H out-of-plane vibrations for substituted naphthalenes: two adjacent hydrogen atoms (◇), four adjacent hydrogen atoms (□), and four adjacent hydrogen atoms in dihydroisoquinoline (○) and out-of-plane ring deformation of disubstituted naphthalenes (△).

bending vibrations of substituted naphthalenes whose positions have been correlated with the number of adjacent hydrogen atoms in the aromatic rings. A common feature in all the fused-ring naphthoxazines synthesized in this study is the presence of two adjacent hydrogen atoms (positions 3 and 4) whose C–H out-of-plane bending vibration can be clearly observed between 816 and 793 cm^{-1} . Additionally, **1N-p-f**, **1N-p6-f**, and **1N-dihq-f** show strong pair of bands between 762 and 735 cm^{-1} which are associated with C–H out-of-plane bending of four adjacent hydrogen atoms (positions 5, 6, 7, and 8). Furthermore, the characteristic band due to out-of-plane ring deformation vibration in disubstituted naphthalenes can be observed centered at 653 cm^{-1} for **1N-p-f**, **1N-p6-f**, and **1N-dihq-f**. The extra bands emerging in the shown region of the FT-IR spectrum of **1N-dihq-f** are associated with the C–H out-of-plane bending vibration of the four adjacent hydrogen atoms in the dihydroisoquinoline moiety of the compound.

Thermal Behavior of Fused-Ring Naphthoxazines. The thermal behavior of the fused-ring naphthoxazines was studied by differential scanning calorimetry. The thermograms of all the compounds are shown in **Figure 4** along with model monofunctional benzoxazine, **PH-a**, that is synthesized from phenol and aniline.

All thermograms show both an endothermic and an exothermic event which are attributed to the melting and ring-opening reaction of the different compounds, respectively. Compared to the polymerization temperature of **PH-a** at $271\text{ }^\circ\text{C}$, the ring-opening reaction temperatures of all the fused-ring naphthoxazines, **1N-p-f**, **1N-p6-f**, and **1N-dihq-f**, are significantly lower, specifically 189 , 192 , and $203\text{ }^\circ\text{C}$, respectively.

It is rather unusual to observe such low ring-opening reaction temperatures in ordinary naphthoxazines and benzoxazines, unless they are somehow influenced by some external or internal driving forces, such as catalytic systems^{30,31} or hydrogen-bond motives^{32,33} inducing such a property. Nevertheless, the reduction of the polymerization temperature might be caused by multiple factors acting simultaneously. For example, a strong basicity of the tertiary amine forming a constitutive part of multicycle aliphatic structure, in addition to an increased ring tension of the oxazine ring due to the presence of the two fused-rings directly attached to it, the

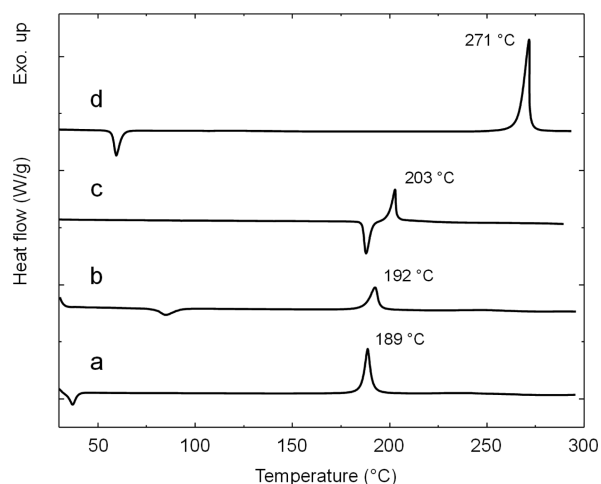


Figure 4. DSC thermograms of (a) 1N-p-f, (b) 1N-p6-f, (c) 1N-dihq-f, and (d) PH-a.

aromatic and the aliphatic ones, might act as internal driving forces toward polymerization.

Ring-Opening Reaction of Fused-Ring Naphthoxazines. FT-IR analysis was also used to study the ring-opening reaction of these compounds. For instance, Figure 5 shows the

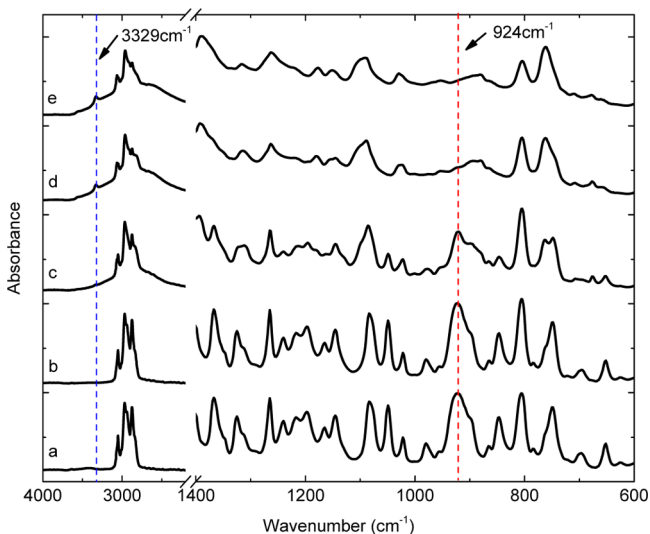


Figure 5. FT-IR spectra of 1N-p-f between the regions 4000–2000 and 1400–600 cm^{-1} at (a) rt, (b) 120 $^{\circ}\text{C}$ for 1 h, (c) 130 $^{\circ}\text{C}$ for 30 min, (d) 140 $^{\circ}\text{C}$ for 30 min, and (e) 150 $^{\circ}\text{C}$ for 30 min. Red and blue dashed lines in the figure indicate where bands disappear and emerge, respectively. Those processes are accompanied by the characteristic splitting of the typical benzoxazine related band, reflecting the C–H out-of-plane bending of the four vicinal aromatic hydrogens in the naphthalene moiety combined with the O–C stretching mode from the O bonded to the C at the 2-position, and other modes as minor contributors.³⁴

FT-IR spectra of a single sample of 1N-p-f at room temperature, which then was consecutively heated at 120 $^{\circ}\text{C}$ for 1 h, 130 $^{\circ}\text{C}$ for 30 min, 140 $^{\circ}\text{C}$ for 30 min, and finally at 150 $^{\circ}\text{C}$ for 30 min.

Characteristic bands associated with oxazine ring clearly vanished as 1N-p-f was subjected to increasing temperatures, namely, 1325, 1240, 1198, 1049, and 924 cm^{-1} (see Table 1 for their assignment). Consequently, the O–H stretching vibration

band of the open-ring structure could clearly be observed emerging at 3329 cm^{-1} . Interestingly, the region in the FT-IR spectra between 900 and 600 cm^{-1} , associated with the out-of-plane C–H bending vibrations of substituted naphthalenes, was also affected with increasing temperature. As the band due to the two adjacent hydrogen atoms (out-of-plane C–H bend.) at 806 cm^{-1} decreased, the pair of bands centered at 755 cm^{-1} , associated with the four adjacent hydrogen atoms (out-of-plane C–H bend.), experienced a clear change in shape. At the same time, a new band of medium-weak nature appeared at 881 cm^{-1} . This band falls into the region associated with the out-of-plane C–H bending of an isolated hydrogen atom in a substituted naphthalene, namely, between 900 and 855 cm^{-1} . Furthermore, the characteristic band due to the out-of-plane ring deformation vibration in disubstituted naphthalenes at 653 cm^{-1} , common in all the fused-ring benzoxazines, decreased as temperature increased. What this seems to suggest is that according to the proposed mechanism of ring-opening reaction of benzoxazine,³⁵ after the ring-opening step, the subsequent electrophilic substitution occurs at the free *para* position (4n-position) of the naphthol. However, the possibility of substitutions in other position than 4n in the naphthalene moiety should not be ignored. Thus, substitution in either the 6n- or 7n-position would also generate bands associated with the out-of-plane C–H bending of both an isolated hydrogen and two adjacent hydrogen atoms. A substitution in either the 5n- or 8n-position would, however, generate new bands in the region 820–730 cm^{-1} due to the out-of-plane C–H bending of three adjacent hydrogen atoms, which were not observed.

Moreover, solid-state ^1H and ^{13}C NMR analyses were carried out to further study the ring-opening polymerization reaction of 1N-p-f. Figure 6 shows solution and solid-state ^1H NMR spectra of 1N-p-f and 1N-p-f under MAS conditions after 5 h at 60 $^{\circ}\text{C}$ and solid-state ^1H MAS NMR of poly(1N-p-f). Although the spectrum of 1N-p-f in Figure 6b shows significant line broadening, three regions can be clearly differentiated, namely, 8.00–6.00, 4.50–3.50, and 2.50–0.50 ppm, whose

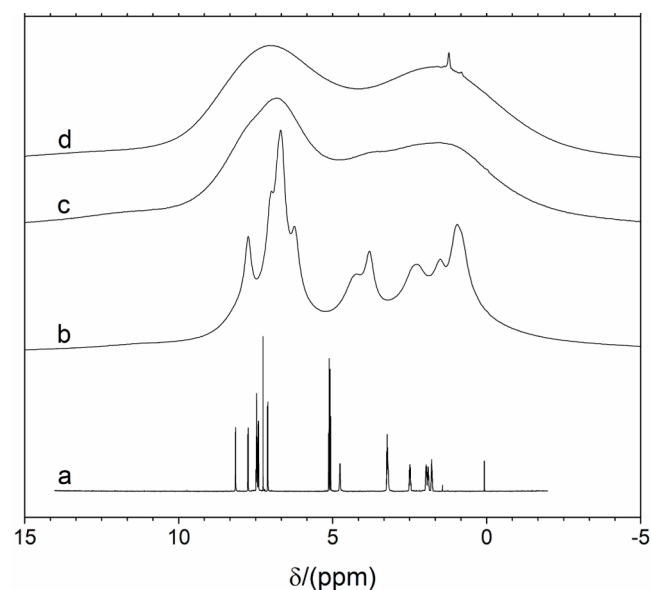


Figure 6. ^1H NMR spectra of (a) 1N-p-f (in solution using deuterated chloroform), (b) 1N-p-f (under MAS at 30 kHz), (c) 1N-p-f after 5 h at 60 $^{\circ}\text{C}$ (under MAS at 30 kHz), and (d) poly(1N-p-f) (under MAS at 30 kHz).

signals can be assigned to the aromatic region, the oxazine ring, and the pyrrolidine moiety protons, respectively. As previously reported,³⁶ there is a constant frequency shift of about 0.9 ppm between the proton signals between the solid and solution-state ¹H NMR spectra. Figure 6c shows the spectrum of 1N-p-f under MAS conditions, where the monomer starts to form bigger structures. Because of their reduced mobility, the ¹H signals broaden in the spectrum substantially, and the spectral resolution of the different ¹H sites is lost. In contrast to the fully reacted polymer (Figure 6d), the new repeat unit shows some resolution in the aromatic region and weak signals in the naphthoxazine ring region between 4.50 and 3.50 ppm, which are not observed in the poly(1N-p-f) sample due to ring-opening polymerization reaction. Figure 7 shows the ¹³C NMR

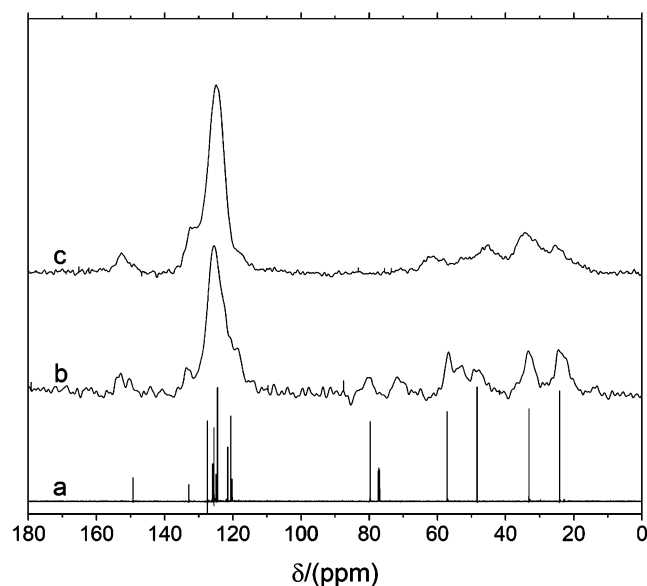


Figure 7. ¹³C NMR spectra of (a) 1N-p-f (in solution using deuterated chloroform), (b) 1N-p-f (after 5 h at 60 °C under MAS at 25 kHz), and (c) poly(1N-p-f) (under MAS at 25 kHz).

spectrum of 1N-p-f and ¹³C CP MAS spectra of both 1N-p-f under MAS condition after 5 h at 60 °C and poly(1N-p-f). By analogy to the solution-state ¹³C NMR spectrum, the carbon signals of the oxazine ring in the ¹³C CP MAS spectrum can be observed at 57 and 80 ppm. The signals between 20 and 49 ppm belong to the pyrrolidine moiety, while the rest of the signals are from the aromatic carbons. Upon polymerization, the carbon signal at 80 ppm, which relates to the 2-position of the oxazine ring, vanished, whereas the carbon signal related to the 4-position shifted from 57 to 62 ppm. Further indication of polymerization reaction can be observed in the changes occurred in the aromatic region, especially in the reduction of the intensity of the signal at 119 ppm, which is assigned to the *para*-activated carbon in the naphthalene moiety at the 4n-position.

Although further detailed analysis will be required to understand the exact structure of the polymer, based on the FT-IR and solid state NMR analyses, the following most likely structure of poly(1N-p-f) in idealized manner can be presented in Figure 8.

Size Exclusion Chromatography (SEC) Analysis. The 1N-p-f model monomer was subjected to heat treatment at 150 °C for 2.5 h. Molecular weight of the heat treated monomer

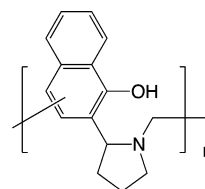


Figure 8. Idealized structure of the polynaphthoxazine, poly(1N-p-f), obtained from heat-treated 1N-p-f.

was measured by SEC in tetrahydrofuran (THF) as the eluent against polystyrene standards. Dynamic light scattering information acquired from SEC presents molecular weight of soluble part of 1N-p-f oligomer resulting from its partial solubility in THF solvent. Results obtained using the ultraviolet detector indicate number-average molecular weight (M_n) and weight-average molecular weight (M_w) of 655 and 909 Da, respectively, for the 1N-p-f oligomer. As can be estimated from the aforementioned results, the degree of oligomerization of 1N-p-f oligomers is about 3 and 4 from the number-average molecular weight and weight-average molecular weight, respectively. This oligomerization behavior is very similar to the well-known small oligomer formation of benzoxazine resins containing only one oxazine ring.^{37,38} Additionally, the complexity of degradation reactions proceed simultaneously with the polymerization of naphthoxazines upon heat treatment and may also contribute to the seemingly lower molecular weight²³ of the fused-ring oligomers. However, it should be noted that the temperature applied to prepare 1N-p-f oligomers was 150 °C, which is significantly lower than the exotherm peak temperature, 189 °C, that was determined from DSC. It is reasonable to extrapolate that larger molecular weight of poly(1N-p-f) with higher heat treatment temperature could be obtained. Because of the aforementioned solubility problem of some fraction of the reacted resin, this low temperature was chosen to unambiguously demonstrate the possibility of polymerization, albeit forming small oligomers. SEC analysis, together with the nonisothermal kinetics acquired by FT-IR, of the 1N-p-f monomer suggests a similar polymerization pathway as the typical benzoxazines. SEC data are summarized in Table 2.

Table 2. SEC Results of Oligomer from 1N-p-f Monomer with Heat Treatment at 150 °C for 2.5 h

| Resin | Detector | M_n (Da) | M_w (Da) | M_w/M_n |
|-------|----------|------------|------------|-----------|
| | IR | 600 | 900 | 1.50 |
| | UV | 650 | 900 | 1.38 |

Thermal Stability. To study the thermal stability of the materials generated upon polymerization of the fused-ring naphthoxazines, the three resins were polymerized under the same conditions. The polymerization cycle for every sample consisted of four consecutive heating steps of 1 h each at the following temperatures; 150, 180, 200, and 220 °C. The resulting materials were studied by thermogravimetric analysis (TGA), and the results are shown in Figure 9.

As can be observed from Figure 9, all polymers obtained upon polymerization of the fused-ring naphthoxazines prepared in this study showed a similar degradation profile. Two main degradation steps are observed from the first-derivative curves

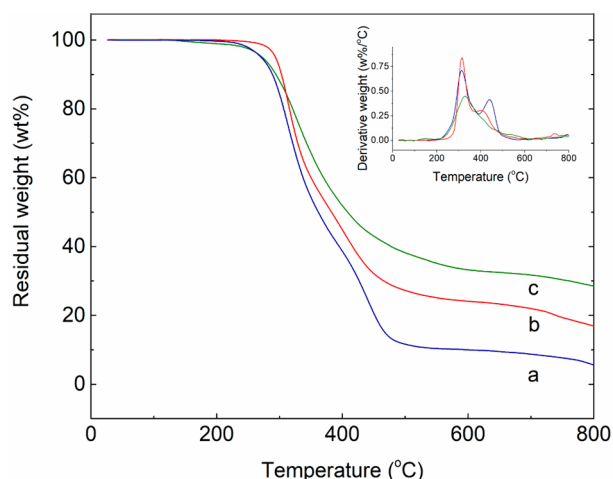
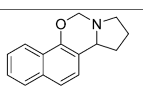
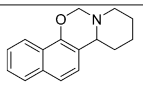
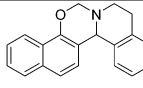


Figure 9. TGA thermograms of (a) poly(1N-p6-f), (b) poly(1N-p-f), and (c) poly(1N-dhiq-f). Inset shows the derivative of the weight loss of poly(1N-p6-f) (green line), poly(1N-p-f) (blue line), and poly(1N-dhiq-f) (red line) as a function of the temperature.

(inset in Figure 9), being the first one where the greater weight loss occurs. There seems to exist an expected pattern in the thermal stability dependency on the aliphatic content of the fused-ring naphthoxazines. Thus, the monomer with the highest aliphatic content, the six-member fused-ring naphthoxazine 1N-p6-f, generates a polymer that produces the lowest char yield of 6%. An outcome that is systematically improved as the aliphatic content diminishes as in poly(1N-p-f) (17%) and even further as in poly(1N-dhiq-f) (28%). The greater thermal stability of poly(1N-dhiq-f) is not only observed in the resulting char yield (28%) but also in both T_{d5} and T_{d10} values of 272 and 294 °C, respectively. Table 3 summarizes the

Table 3. Thermal Properties of Polymerized Fused-Ring Naphthoxazine Resins

| Monomer | Polymers | T_{d5} (°C) | T_{d10} (°C) | Char yield (%) |
|---|-----------------|---------------|----------------|----------------|
|  | poly(1N-p-f) | 293 | 303 | 17 |
|  | poly(1N-p6-f) | 271 | 369 | 6 |
|  | poly(1N-dhiq-f) | 272 | 294 | 28 |

thermal stability values of the polymers. These results offer high probability of greatly improved thermal stability once the di- or multifunctional fused-ring naphthoxazines are studied, in an analogous manner as the improvement from monofunctional to difunctional benzoxazine resins. The study for multifunctional fused-ring naphthoxazines and benzoxazines will be reported in time elsewhere.

CONCLUSION

Polymerization of fused-ring naphthoxazines was reported for the first time. Strong evidence supporting polymerization behavior of this class of compounds was obtained by FT-IR in

cumulative heating experiments, indicating a similar ring-opening reaction upon thermal polymerization. Together with the thermal behavior investigation by DSC studies, a significantly lower polymerization temperature than traditional benzoxazine monomers was confirmed for this novel class of resins, namely fused-ring naphthoxazines.

AUTHOR INFORMATION

Corresponding Authors

*E-mail: hxi3@case.edu (H.I.).

*E-mail: pxf106@case.edu (P.F.).

ORCID

Hatsuo Ishida: 0000-0002-2590-2700

Notes

The authors declare no competing financial interest.

REFERENCES

- (1) Nair, C. P. R. Advances in addition-cure phenolic resins. *Prog. Polym. Sci.* **2004**, *29*, 401–498.
- (2) Ishida, H.; Froimowicz, P. *Advanced and Emerging Polybenzoxazine Science and Technology*; Elsevier: Amsterdam, 2017.
- (3) Ishida, H.; Allen, D. J. Physical and mechanical characterization of near-zero shrinkage polybenzoxazines. *J. Polym. Sci., Part B: Polym. Phys.* **1996**, *34*, 1019–1030.
- (4) Agag, T.; Takeichi, T. Synthesis and characterization of novel benzoxazine monomers containing allyl groups and their high performance thermosets. *Macromolecules* **2003**, *36*, 6010–6017.
- (5) Froimowicz, P.; Arza, C. R.; Han, L.; Ishida, H. Smart, Sustainable, and Ecofriendly Chemical Design of Fully Bio-Based Thermally Stable Thermosets Based on Benzoxazine Chemistry. *ChemSusChem* **2016**, *9*, 1921–1928.
- (6) Espinosa, M. A.; Galia, M.; Cadiz, V. Novel phosphorilated flame retardant thermosets: epoxy-benzoxazine-novolac systems. *Polymer* **2004**, *45*, 6103–6109.
- (7) Froimowicz, P.; Arza, C. R.; Ohashi, S.; Ishida, H. Tailor-Made and Chemically Designed Synthesis of Coumarin-Containing Benzoxazines and Their Reactivity Study Toward Their Thermosets. *J. Polym. Sci., Part A: Polym. Chem.* **2016**, *54*, 1428–1435.
- (8) Ishida, H.; Low, H. Y. A study on the volumetric expansion of benzoxazine-based phenolic resin. *Macromolecules* **1997**, *30*, 1099–1106.
- (9) Wang, C. F.; Su, Y. C.; Kuo, S. W.; Huang, C. F.; Sheen, Y. C.; Chang, F. C. Low-surface-free-energy materials based on polybenzoxazines. *Angew. Chem., Int. Ed.* **2006**, *45*, 2248–2251.
- (10) Yagci, Y.; Kiskan, B.; Ghosh, N. N. Recent advancement on polybenzoxazine-A newly developed high performance thermoset. *J. Polym. Sci., Part A: Polym. Chem.* **2009**, *47*, 5565–5576.
- (11) Andreu, R.; Ronda, J. C. Synthesis of 3,4-Dihydro-2H-1,3-benzoxazines by Condensation of 2-Hydroxyaldehydes and Primary Amines: Application to the Synthesis of Hydroxy-Substituted and Deuterium-Labeled Compounds. *Synth. Commun.* **2008**, *38*, 2316–2329.
- (12) Lin, C. H.; Lin, H. T.; Chang, S. L.; Hwang, H. J.; Hu, Y. M.; Taso, Y. R.; Su, W. C. Benzoxazines with tolyl, p-hydroxyphenyl or p-carboxyphenyl linkage and the structure–property relationship of resulting thermosets. *Polymer* **2009**, *50*, 2264–2272.
- (13) Liu, Y.-X.; Ma, H.-M.; Liu, Y.; Qiu, J.-J.; Liu, C.-M. A well-defined poly(vinyl benzoxazine) obtained by selective free radical polymerization of vinyl group in bifunctional benzoxazine monomer. *Polymer* **2016**, *82*, 32–39.
- (14) Ohashi, S.; Kilbane, J.; Heyl, T.; Ishida, H. Synthesis and Characterization of Cyanate Ester Functional Benzoxazine and Its Polymer. *Macromolecules* **2015**, *48*, 8412–8417.
- (15) Kaji, M.; Endo, T. Synthesis of a novel epoxy resin containing naphthalene moiety and properties of its cured polymer with phenol novolac. *J. Polym. Sci., Part A: Polym. Chem.* **1999**, *37*, 3063–3069.

- (16) Ohno, M.; Takata, T.; Endo, T. Synthesis of a Novel Naphthalene-Based Poly(arylene ether ketone) with High Solubility and Thermal Stability. *Macromolecules* **1994**, *27*, 3447–3448.
- (17) Liaw, D. J.; Chang, F. C.; Leung, M. K.; Chou, M. Y.; Muellen, K. High Thermal Stability and Rigid Rod of Novel Organosoluble Polyimides and Polyamides Based on Bulky and Noncoplanar Naphthalene-Biphenyldiamine. *Macromolecules* **2005**, *38*, 4024–4029.
- (18) Kiskan, B.; Yagci, Y. Synthesis and characterization of naphthoxazine functional poly(*ε*-caprolactone). *Polymer* **2005**, *46*, 11690–11697.
- (19) Wang, C.-S.; Hwang, H.-J. Investigation of bismaleimide containing naphthalene unit. II. Thermal behavior and properties of polymer. *J. Polym. Sci., Part A: Polym. Chem.* **1996**, *34*, 1493–1500.
- (20) Shen, S. B.; Ishida, H. Synthesis and Characterization of Polyfunctional Naphthoxazines and Related Polymers. *J. Appl. Polym. Sci.* **1996**, *61*, 1595–1605.
- (21) Uyar, T.; Koyuncu, Z.; Ishida, H.; Hacıoğlu, J. Polymerisation and degradation of an aromatic amine-based naphthoxazine. *Polym. Degrad. Stab.* **2008**, *93*, 2096–2103.
- (22) Yildirim, A.; Kiskan, B.; Demirel, A. L.; Yagci, Y. Synthesis, characterization and properties of naphthoxazine-functional poly(propyleneoxide)s. *Eur. Polym. J.* **2006**, *42*, 3006–3014.
- (23) Uyar, T.; Hacıoğlu, J.; Ishida, H. Synthesis, characterization, and thermal properties of alkyl-functional naphthoxazines. *J. Appl. Polym. Sci.* **2013**, *127*, 3114–3123.
- (24) Ohashi, S.; Pandey, V.; Arza, C. R.; Froimowicz, P.; Ishida, H. Simple and low energy consuming synthesis of cyanate ester functional naphthoxazines and their properties. *Polym. Chem.* **2016**, *7*, 2245–2252.
- (25) Heydenreich, M.; Koch, A.; Szatmári, I.; Fülöp, F.; Kleinpeter, E. Synthesis and conformational analysis of naphth[1,2-*e*][1,3]oxazino[4,3-*a*][1,3]isoquinoline and naphth[2,1-*e*][1,3]oxazino[4,3-*a*]isoquinoline derivatives. *Tetrahedron* **2008**, *64*, 7378–7385.
- (26) Deb, M. L.; Dey, S. S.; Bento, I.; Barros, M. T.; Maycock, C. D. Copper-catalyzed regioselective intramolecular oxidative alpha-functionalization of tertiary amines: an efficient synthesis of dihydro-1,3-oxazines. *Angew. Chem., Int. Ed.* **2013**, *52*, 9791–5.
- (27) Mahato, S.; Haldar, S.; Jana, C. K. Diastereoselective alpha-C-H functionalization of aliphatic N-heterocycles: an efficient route to ring fused oxazines. *Chem. Commun. (Cambridge, U. K.)* **2014**, *50*, 332–4.
- (28) Gravel, E.; Poupon, E.; Hocquemiller, R. Biomimetic investigations from reactive lysine-derived C5 units: one step synthesis of complex polycyclic alkaloids from the Nitraria genus. *Tetrahedron* **2006**, *62*, 5248–5253.
- (29) Cimarelli, C.; Fratoni, D.; Mazzanti, A.; Palmieri, G. Betti Reaction of Cyclic Imines with Naphthols and Phenols - Preparation of New Derivatives of Betti's Bases. *Eur. J. Org. Chem.* **2011**, *2011*, 2094–2100.
- (30) Andreu, R.; Reina, J. A.; Ronda, J. C. Carboxylic acid-containing benzoxazines as efficient catalysts in the thermal polymerization of benzoxazines. *J. Polym. Sci., Part A: Polym. Chem.* **2008**, *46*, 6091–6101.
- (31) Zhang, W. F.; Froimowicz, P.; Arza, C. R.; Ohashi, S.; Xin, Z.; Ishida, H. Latent Catalyst-Containing Naphthoxazine: Synthesis and Effects on Ring-Opening Polymerization. *Macromolecules* **2016**, *49*, 7129–7140.
- (32) Froimowicz, P.; Zhang, K.; Ishida, H. Intramolecular Hydrogen Bonding in Benzoxazines: When Structural Design Becomes Functional. *Chem. - Eur. J.* **2016**, *22*, 2691–2707.
- (33) Zhang, K.; Ishida, H. An anomalous trade-off effect on the properties of smart ortho-functional benzoxazines. *Polym. Chem.* **2015**, *6*, 2541–2550.
- (34) Han, L.; Iguchi, D.; Gil, P.; Heyl, T. R.; Sedwick, V. M.; Arza, C. R.; Ohashi, S.; Lacks, D. J.; Ishida, H. Oxazine Ring-Related Vibrational Modes of Benzoxazine Monomers Using Fully Aromatically Substituted, Deuterated, N-15 Isotope Exchanged, and Oxazine-Ring-Substituted Compounds and Theoretical Calculations. *J. Phys. Chem. A* **2017**, *121*, 6269–6282.
- (35) Chutayothin, P.; Ishida, H. Cationic Ring-Opening Polymerization of 1,3-Benzoxazines: Mechanistic Study Using Model Compounds. *Macromolecules* **2010**, *43*, 4562–4572.
- (36) Schnell, I.; Brown, S. P.; Low, H. Y.; Ishida, H.; Spiess, H. W. An investigation of hydrogen bonding in benzoxazine dimers by fast magic-angle spinning and double-quantum H-1 NMR spectroscopy. *J. Am. Chem. Soc.* **1998**, *120*, 11784–11795.
- (37) Laobuthee, A.; Chirachanchai, S.; Ishida, H.; Tashiro, K. Asymmetric mono-oxazine: An inevitable product from Mannich reaction of benzoxazine dimers. *J. Am. Chem. Soc.* **2001**, *123*, 9947–9955.
- (38) Chirachanchai, S.; Laobuthee, A.; Phongtamrug, S. Self Termination of Ring Opening Reaction of p-Substituted Phenol-Based Benzoxazines: An Obstructive Effect via Intramolecular Hydrogen Bond. *J. Heterocycl. Chem.* **2009**, *46*, 714–721.